Electronic Supplementary Material (ESI) for Journal of Materials Chemistry B.

Supporting Information

Heavy-Atom-Free BODIPY Dendrimer: Utilizing the Spin-Vibronic Coupling Mechanism for Two-Photon Photodynamic Therapy in Zebrafish

Lingfeng Wang, Ying Qian*

School of Chemistry and Chemical Engineering, Southeast University, Nanjing, 211189, China

Contents

1. The ^{1}H NMR spectra, ^{13}C NMR spectra and mass spectrometry of AM-BDP, TM-BDP, AM_2-BDP, TM_2-BDP and TM_4-BDP (Fig.S1-S15)

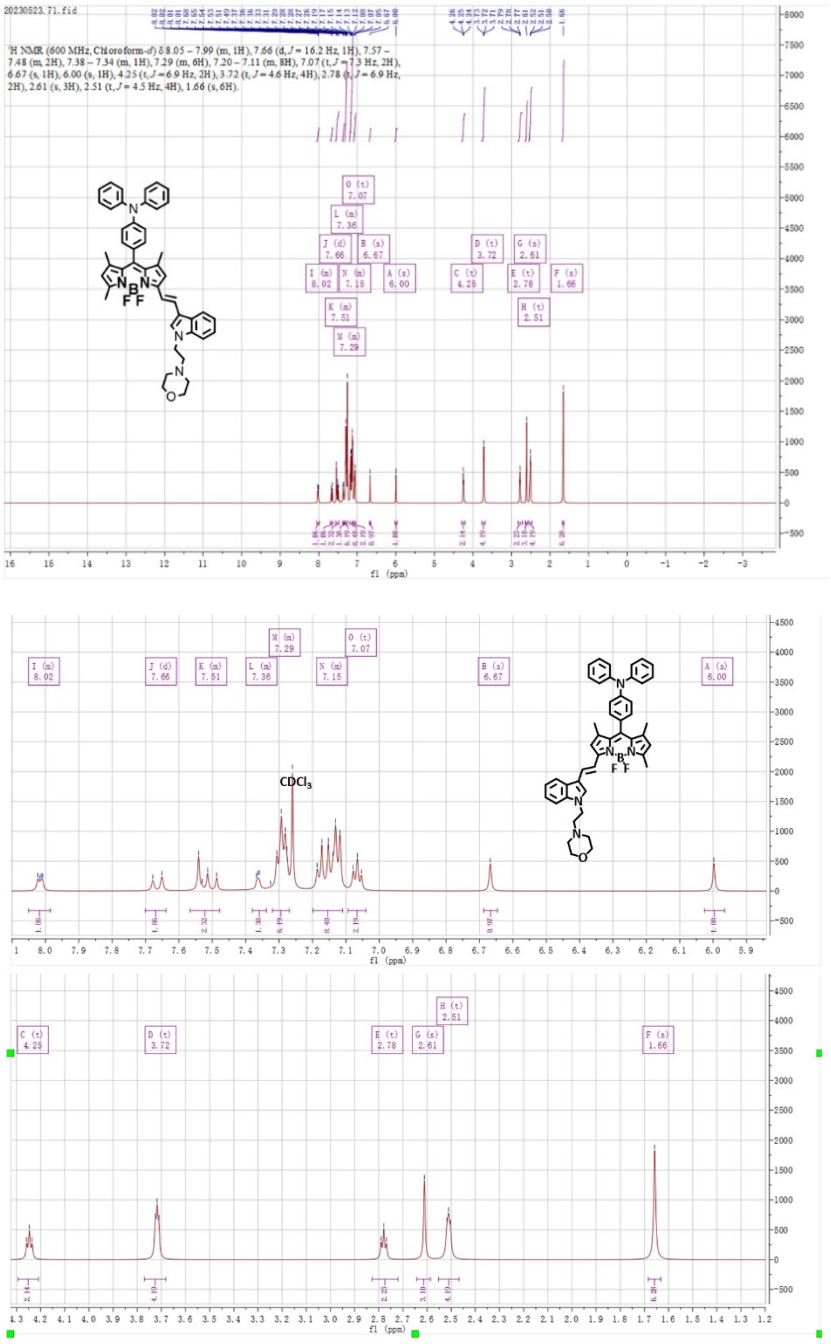

^{1}H NMR (600 MHz, Chloroform-*d*) δ 8.05 – 7.99 (m, 1H), 7.66 (d, *J* = 16.2 Hz, 1H), 7.57 – 7.48 (m, 2H), 7.38 – 7.34 (m, 1H), 7.29 (m, 6H), 7.20 – 7.11 (m, 8H), 7.07 (t, *J* = 7.3 Hz, 2H), 6.67 (s, 1H), 6.00 (s, 1H), 4.25 (t, *J* = 6.9 Hz, 2H), 3.72 (t, *J* = 4.6 Hz, 4H), 2.78 (t, *J* = 6.9 Hz, 2H), 2.61 (s, 3H), 2.51 (t, *J* = 4.5 Hz, 4H), 1.66 (s, 6H).

Fig S1. The ^{1}H NMR spectra of TM-BDP with its' zoomed-in view.

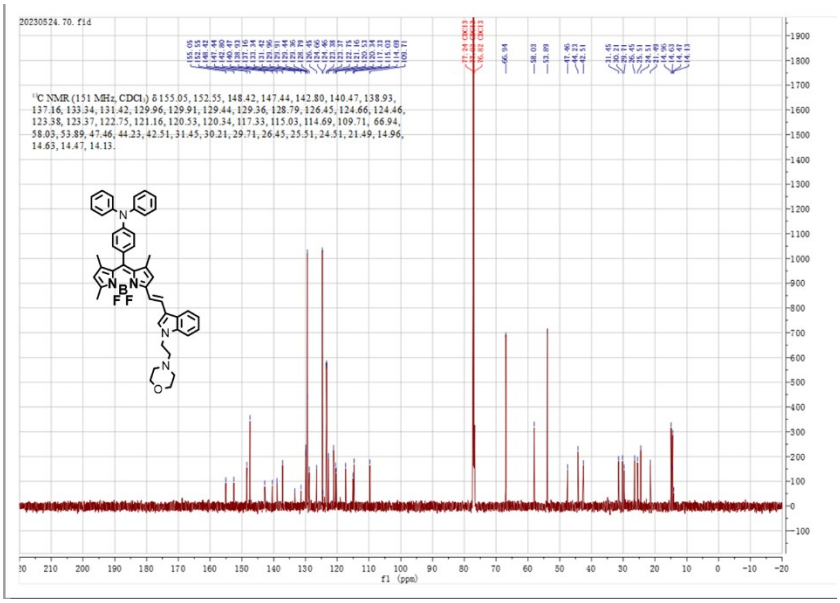

^{13}C NMR (151 MHz, $CDCl_3$) δ 155.05, 152.55, 148.42, 147.44, 142.80, 140.47, 138.93, 137.16, 133.34, 131.42, 129.96, 129.91, 129.44, 129.36, 128.79, 126.45, 124.66, 124.46, 123.38, 123.37, 122.75, 121.16, 120.53, 120.34, 117.33, 115.03, 114.69, 109.71, 66.94, 58.03, 53.89, 47.46, 44.23, 42.51, 31.45, 30.21, 29.71, 26.45, 25.51, 24.51, 21.49, 14.96, 14.63, 14.47, 14.13.

Fig S2. The ^{13}C NMR spectra of TM-BDP.

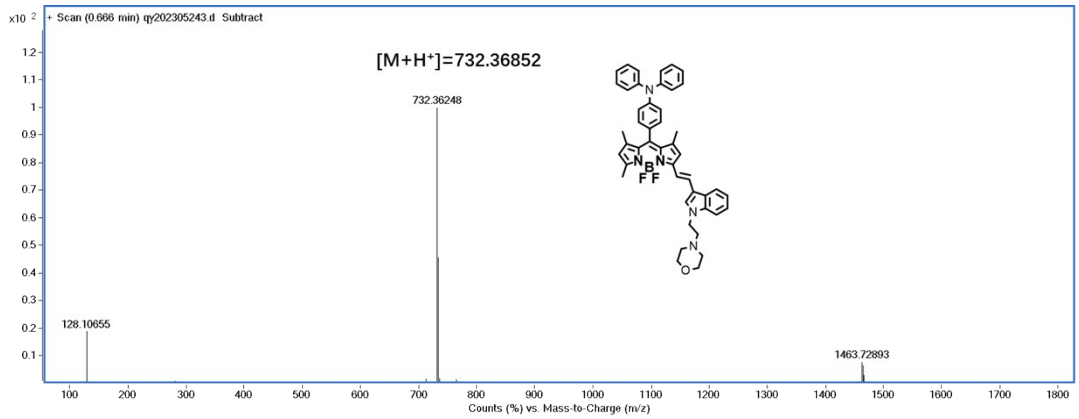

Fig S3. The Mass spectra of TM-BDP.

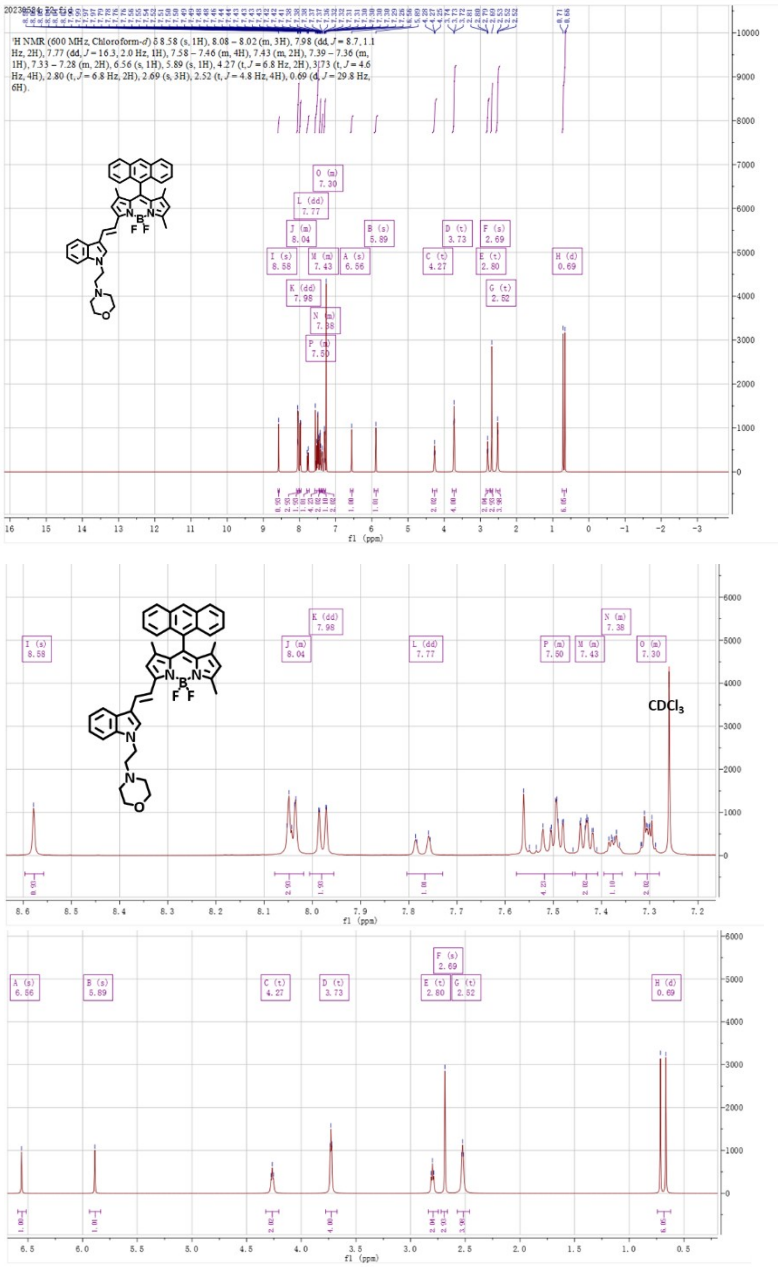

^{1}H NMR (600 MHz, Chloroform-*d*) δ 8.58 (s, 1H), 8.08 – 8.02 (m, 3H), 7.98 (dd, *J* = 8.7, 1.1 Hz, 2H), 7.77 (dd, *J* = 16.3, 2.0 Hz, 1H), 7.58 – 7.46 (m, 4H), 7.43 (m, 2H), 7.39 – 7.36 (m, 1H), 7.33 – 7.28 (m, 2H), 6.56 (s, 1H), 5.89 (s, 1H), 4.27 (t, *J* = 6.8 Hz, 2H), 3.73 (t, *J* = 4.6 Hz, 4H), 2.80 (t, *J* = 6.8 Hz, 2H), 2.69 (s, 3H), 2.52 (t, *J* = 4.8 Hz, 4H), 0.69 (d, *J* = 29.8 Hz, 6H).

Fig S4. The ^{1}H NMR spectra of AM-BDP with its' zoomed-in view.

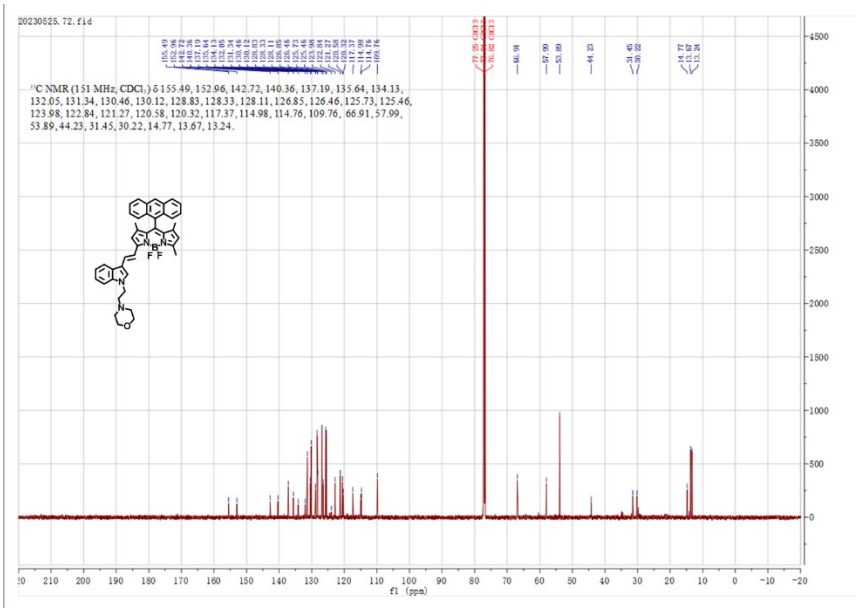

^{13}C NMR (151 MHz, $CDCl_3$) δ 155.49, 152.96, 142.72, 140.36, 137.19, 135.64, 134.13, 132.05, 131.34, 130.46, 130.12, 128.83, 128.33, 128.11, 126.85, 126.46, 125.73, 125.46, 123.98, 122.84, 121.27, 120.58, 120.32, 117.37, 114.98, 114.76, 109.76, 66.91, 57.99, 53.89, 44.23, 31.45, 30.22, 14.77, 13.67, 13.24.

Fig S5. The ^{13}C NMR spectra of AM-BDP.

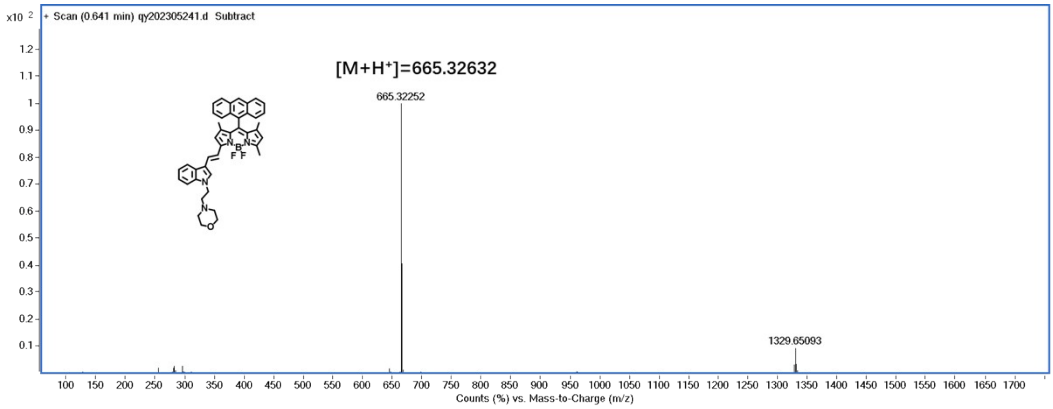

Fig S6. The Mass spectra of AM-BDP.

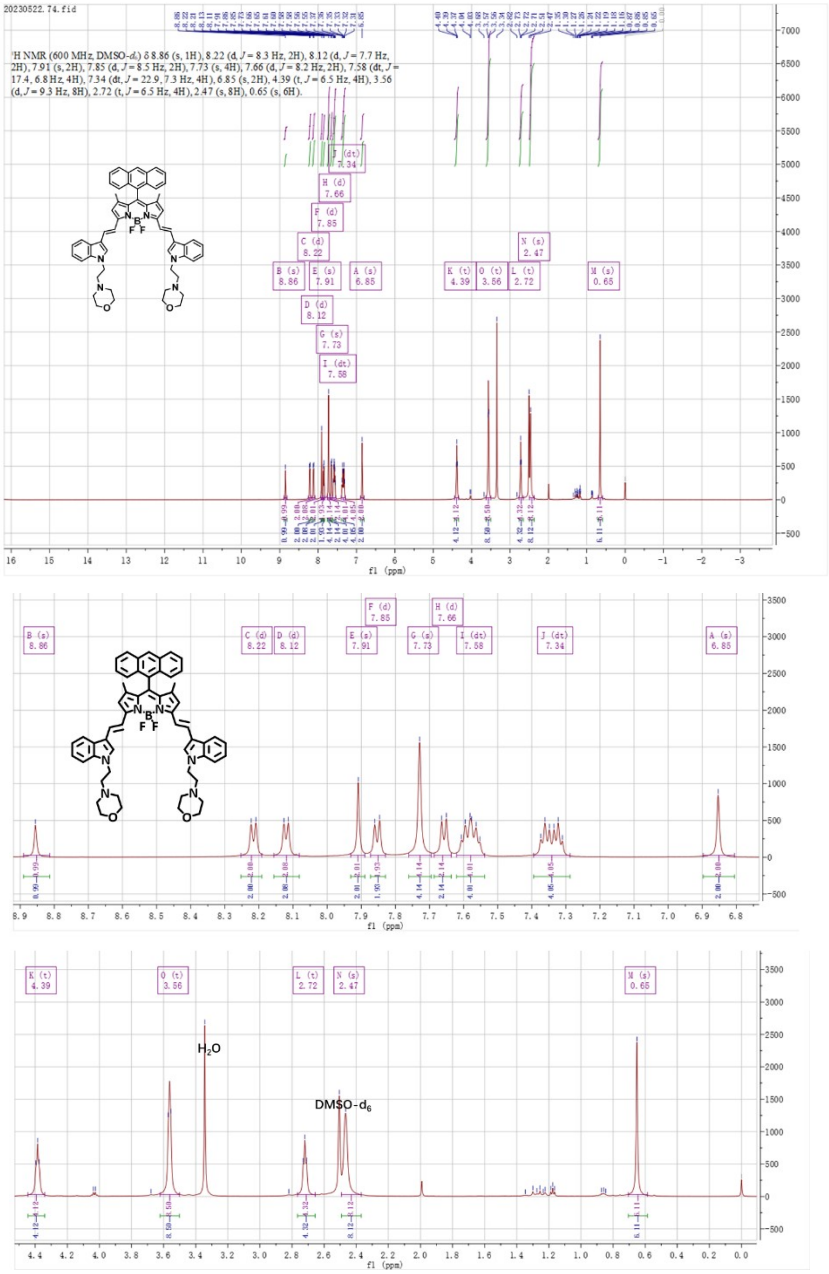

^{1}H NMR (600 MHz, DMSO-d_6) δ 8.86 (s, 1H), 8.22 (d, *J* = 8.3 Hz, 2H), 8.12 (d, *J* = 7.7 Hz, 2H), 7.91 (s, 2H), 7.85 (d, *J* = 8.5 Hz, 2H), 7.73 (s, 4H), 7.66 (d, *J* = 8.2 Hz, 2H), 7.58 (dt, *J* = 17.4, 6.8 Hz, 4H), 7.34 (dt, *J* = 22.9, 7.3 Hz, 4H), 6.85 (s, 2H), 4.39 (t, *J* = 6.5 Hz, 4H), 3.56 (t, *J* = 9.3 Hz, 8H), 2.72 (t, *J* = 6.5 Hz, 4H), 2.47 (s, 8H), 0.65 (s, 6H).

Fig S7. The ^{1}H NMR spectra of AM_2-BDP with its' zoomed-in view.

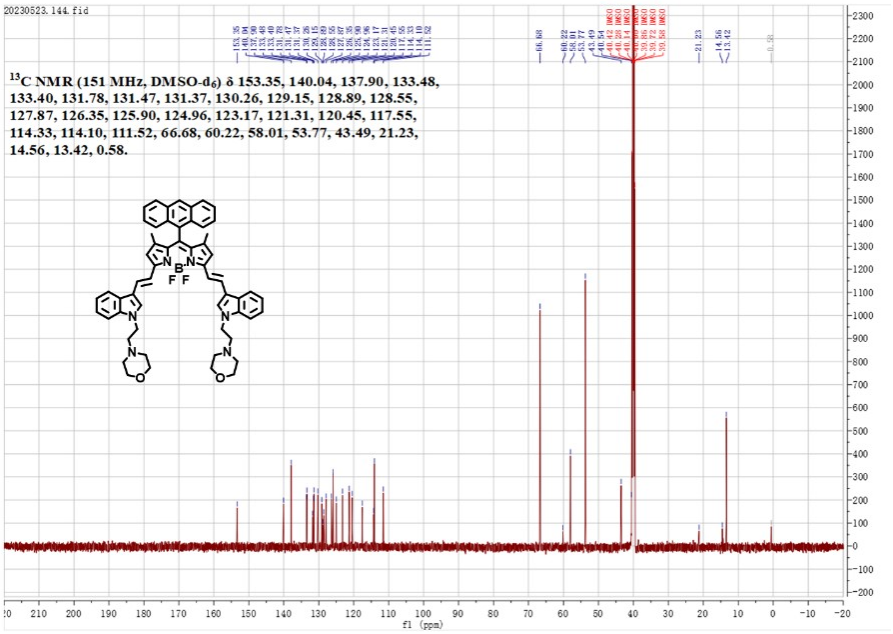

^{13}C NMR (151 MHz, DMSO-d_6) δ 153.35, 140.04, 137.90, 133.48, 133.40, 131.78, 131.47, 131.37, 130.26, 129.15, 128.89, 128.55, 127.87, 126.35, 125.90, 124.96, 123.17, 121.31, 120.45, 117.55, 114.33, 114.10, 111.52, 66.68, 60.22, 58.01, 53.77, 43.49, 21.23, 14.56, 13.42.

Fig S8. The ^{13}C NMR spectra of AM_2-BDP.

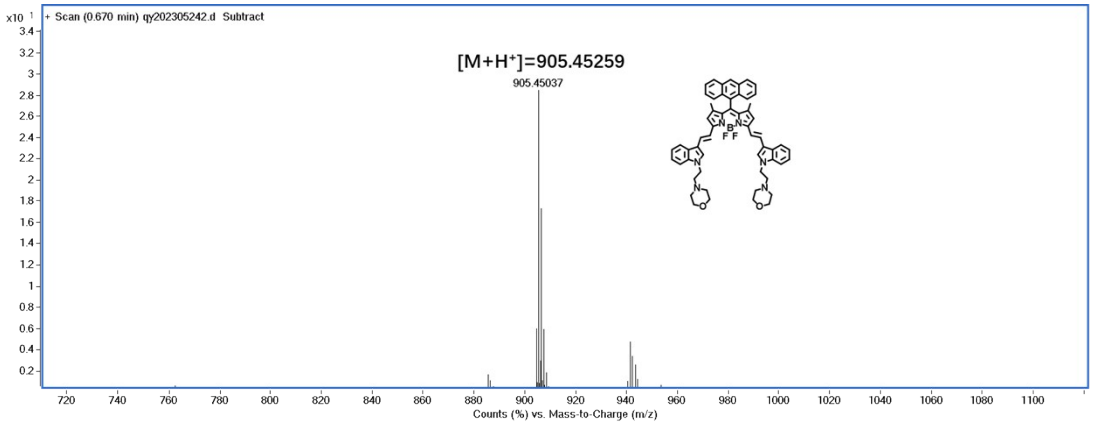

Fig S9. The mass spectra of AM_2-BDP.

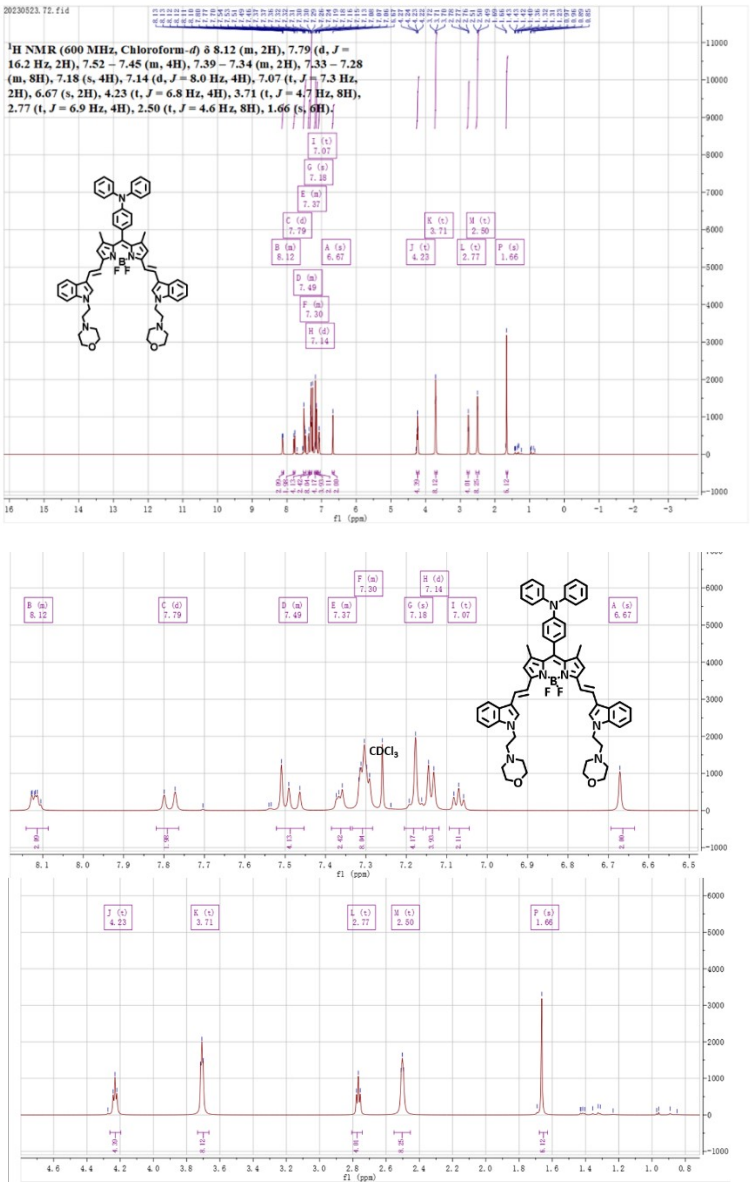

^{1}H NMR (600 MHz, Chloroform-*d*) δ 8.12 (m, 2H), 7.79 (d, *J* = 16.2 Hz, 2H), 7.52 – 7.45 (m, 4H), 7.39 – 7.34 (m, 2H), 7.33 – 7.28 (m, 8H), 7.18 (s, 4H), 7.14 (d, *J* = 8.0 Hz, 4H), 7.07 (t, *J* = 7.3 Hz, 2H), 6.67 (s, 2H), 4.23 (t, *J* = 6.8 Hz, 4H), 3.71 (t, *J* = 4.7 Hz, 8H), 2.77 (t, *J* = 6.9 Hz, 4H), 2.50 (t, *J* = 4.6 Hz, 8H), 1.66 (s, 6H).

Fig S10. The mass spectra of TM_2-BDP with its' zoomed-in view.

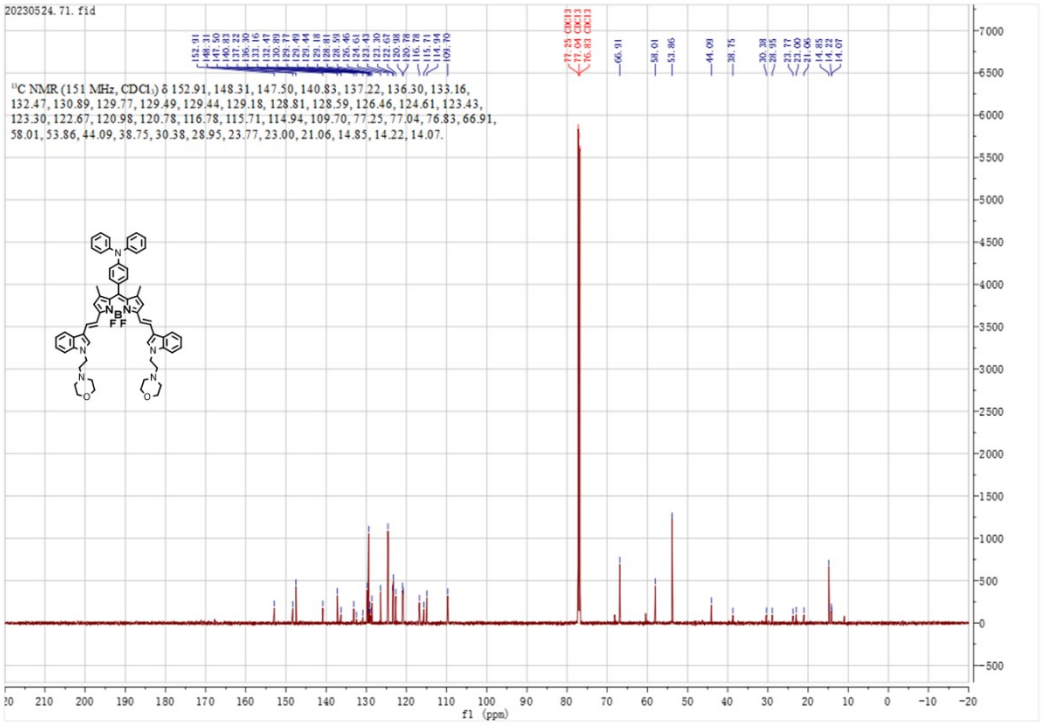

^{13}C NMR (151 MHz, $CDCl_3$) δ 152.91, 148.31, 147.50, 140.83, 137.22, 136.30, 133.16, 132.47, 130.89, 129.77, 129.49, 129.44, 129.18, 128.81, 128.59, 126.46, 124.61, 123.43, 123.30, 122.67, 120.98, 120.78, 116.78, 115.71, 114.94, 109.70, 77.25, 77.04, 76.83, 66.91, 58.01, 53.86, 44.09, 38.75, 30.38, 28.95, 23.77, 23.00, 21.06, 14.85, 14.22, 14.07.

Fig S11. The ^{13}C NMR spectra of TM_2-BDP.

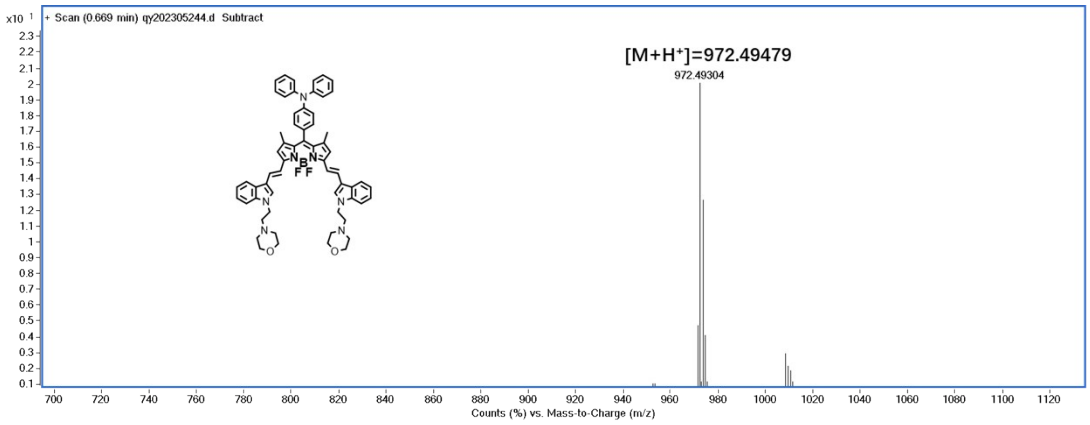

Fig S12. The Mass spectra of TM_2-BDP.

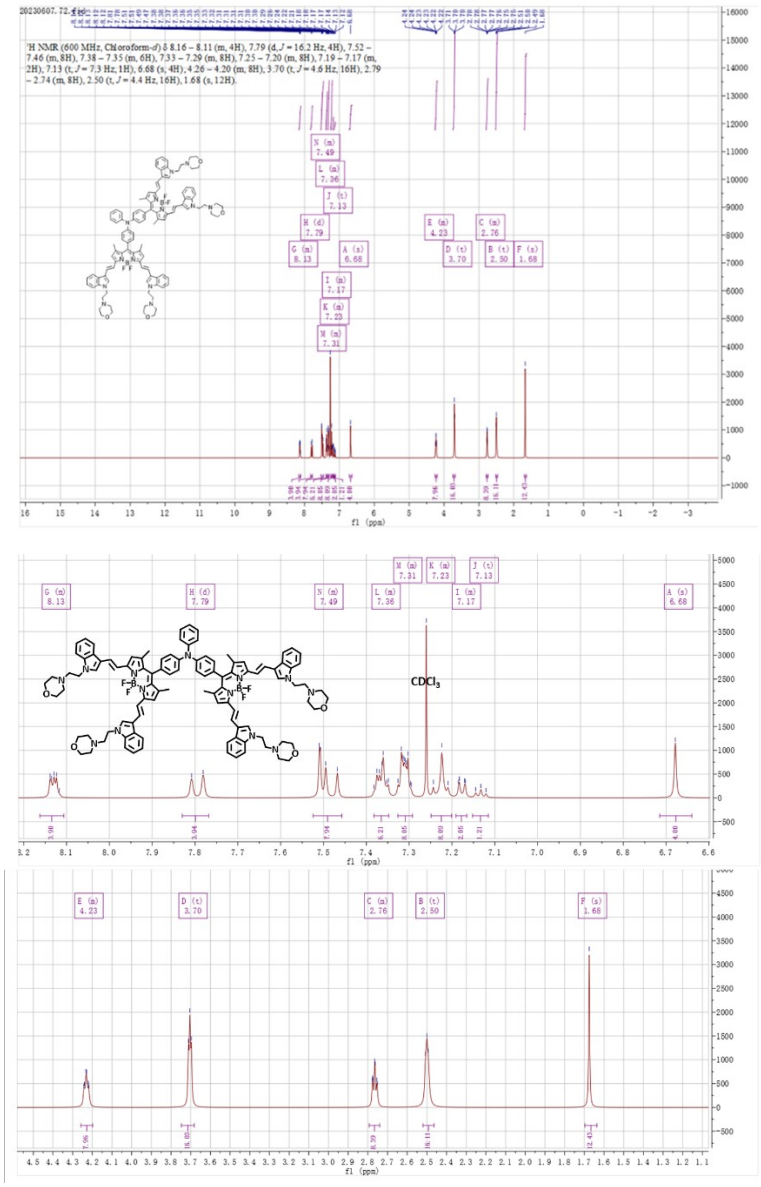

^{1}H NMR (600 MHz, Chloroform-*d*) δ 8.16 – 8.11 (m, 4H), 7.79 (d, *J* = 16.2 Hz, 4H), 7.52 – 7.46 (m, 8H), 7.38 – 7.35 (m, 6H), 7.33 – 7.29 (m, 8H), 7.25 – 7.20 (m, 8H), 7.19 – 7.17 (m, 2H), 7.13 (t, *J* = 7.3 Hz, 1H), 6.68 (s, 4H), 4.26 – 4.20 (m, 8H), 3.70 (t, *J* = 4.6 Hz, 16H), 2.79 – 2.74 (m, 8H), 2.50 (t, *J* = 4.4 Hz, 16H), 1.68 (s, 12H).

Fig S13. The ^{1}H NMR spectra of TM_4-BDP with its' zoomed-in view.

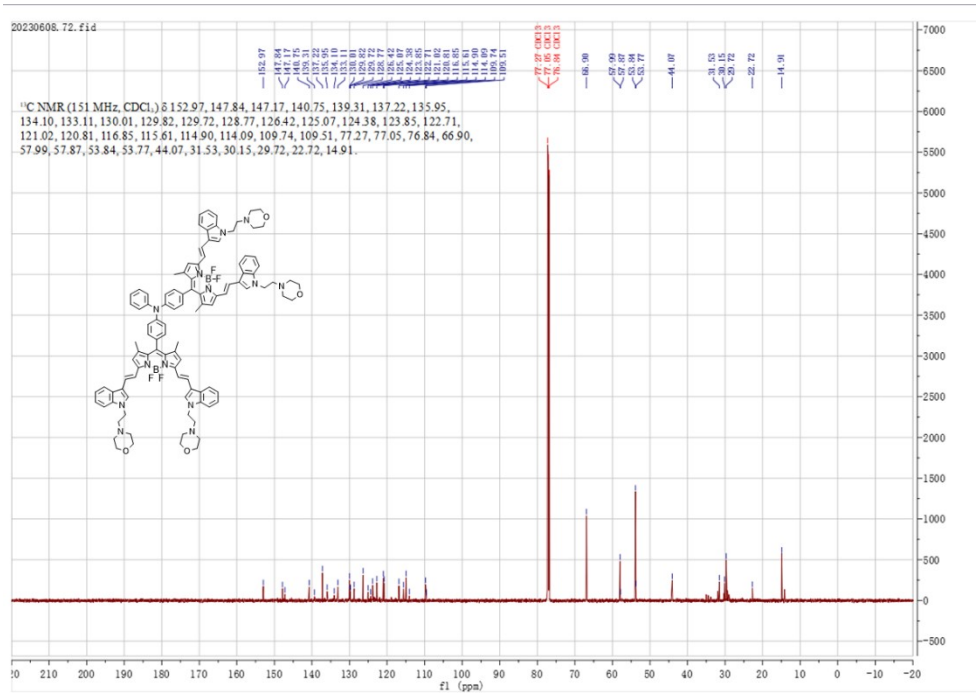

^{13}C NMR (151 MHz, $CDCl_3$) δ 152.97, 147.84, 147.17, 140.75, 139.31, 137.22, 135.95, 134.10, 133.11, 130.01, 129.82, 129.72, 128.77, 126.42, 125.07, 124.38, 123.85, 122.71, 121.02, 120.81, 116.85, 115.61, 114.90, 114.09, 109.74, 109.51, 77.27, 77.05, 76.84, 66.90, 57.99, 57.87, 53.84, 53.77, 44.07, 31.53, 30.15, 29.72, 22.72, 14.91.

Fig S14. The ^{13}C NMR spectra of TM_4-BDP.

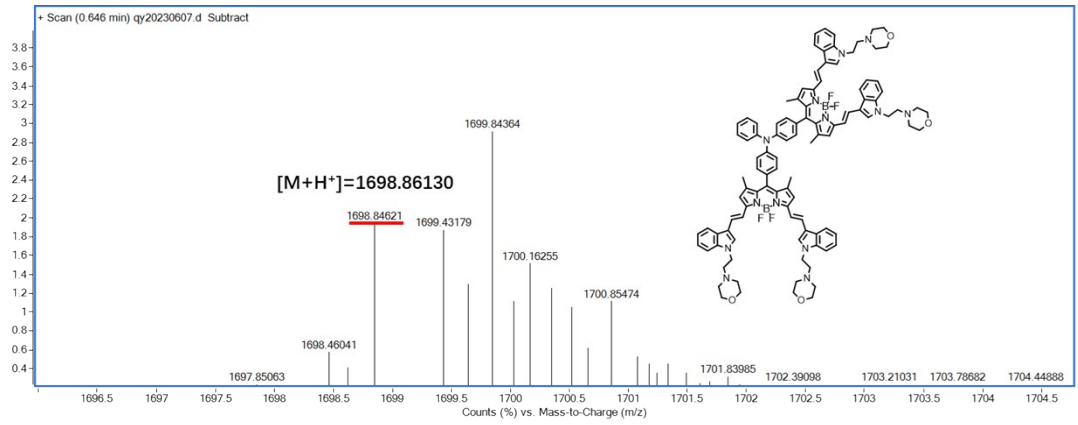

Fig S15. The Mass spectra of TM_4-BDP.

2. The synthesis method of AM-BDP, TM-BDP, AM_2-BDP, TM_2-BDP and TM_4-BDP.

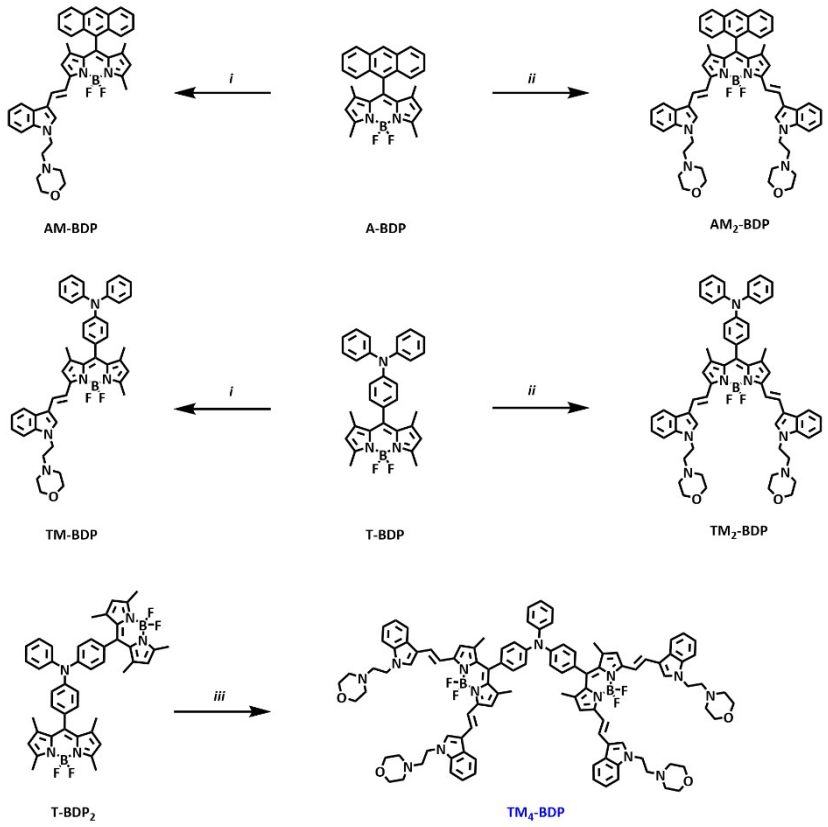

Fig. S16 The synthetic method of the TM_4-BDP dendrimer with its four derivatives, Reagents and conditions: (i) 1-(2-morpholinoethyl)-1H-indole-3-carbaldehyde, acetic acid, piperidine, toluene, refluxed at 110 °C for 4 h. (ii) same reagents with (i), refluxed at 110 °C for 8 h. (iii) same reagents with (i), refluxed at 110 °C for 6 h.

The A-BDP[1, 2], $T\text{-}BDP_1$[3] , $T\text{-}BDP_2$[4] and 1-(2-morpholinoethyl)-1H-indole-3-carbaldehyde(M-CHO) were synthesized according to the reported synthesis method and the AM-BDP, TM-BDP, AM_2-BDP, TM_2-BDP and TM_4-BDP was synthesized through the Knoevenagel reaction. The general procedure and the dosage used in the reaction was described as followed.

General procedure:

The A-BDP/T-BDP/$T\text{-}BDP_2$ and 1-(2-morpholinoethyl)-1H-indole-3-carbaldehyde was added into a 100mL two-necked flask. Then, 15 mL toluene was added and nitrogen was injected for 20 min to ensure that there is no oxygen in the system. Then the corresponding equivalent of piperidine and acetic acid were added, and the time interval between adding the two catalysts was about 1 min. After the reaction system was stirred evenly, then, the reaction temperature was raised to 110℃ and the

reaction was detected by TLC. After the reaction stop, the solvent was dried and the final product was obtained by chromatographic column.

Reactant dosage and reaction time:

AM-BDP: A-BDP (100 mg, 0.236 mmol), 1-(2-morpholinoethyl)-1H-indole-3-carbaldehyde(153 mg, 0.593 mmol), acetic acid (50 μL), piperidine (50 μL), 4 h, obtain: 36.3 mg yield :23.2 %.

AM_2-BDP: A-BDP (100 mg, 0.236 mmol), 1-(2-morpholinoethyl)-1H-indole-3-carbaldehyde(306 mg, 1.186mmol), acetic acid (100 μL), piperidine (100 μL), 8 h, obtain: 90.6 mg yield :42.5 %.

TM-BDP: T-BDP (100 mg, 0.204 mmol), 1-(2-morpholinoethyl)-1H-indole-3-carbaldehyde(159 mg, 0.616 mmol), acetic acid (50 μL), piperidine (50 μL), 4 h, obtain: 22.9 mg yield :15.4 %.

TM_2-BDP: T-BDP (100 mg, 0.204 mmol), 1-(2-morpholinoethyl)-1H-indole-3-carbaldehyde(318 mg, 1.228 mmol), acetic acid (100 μL), piperidine (100 μL), 8 h, obtain: 63.9 mg yield :32.3 %.

TM_4-BDP: $T\text{-}BDP_2$ (50 mg, 0.068 mmol), 1-(2-morpholinoethyl)-1H-indole-3-carbaldehyde(176 mg, 0.682 mmol), acetic acid (100 μL), piperidine (100 μL), 6 h, obtain: 19.8 mg yield:17.2 %.

3. The singlet oxygen yield test of the TM-BDP in different solvent

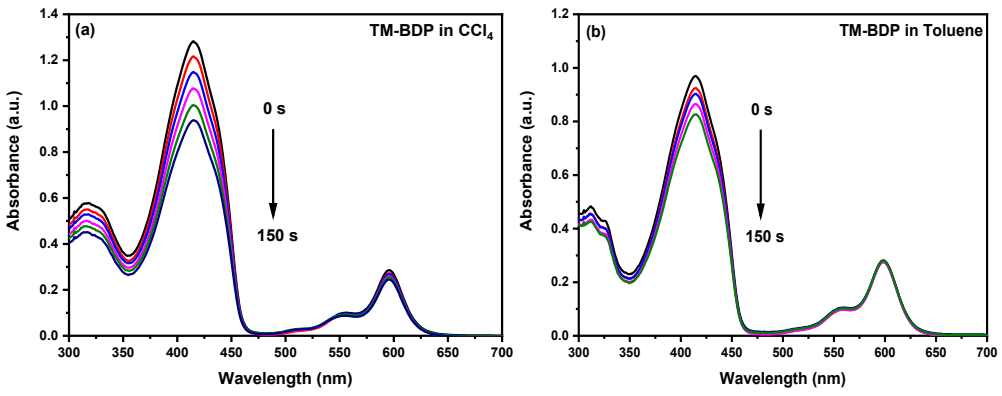

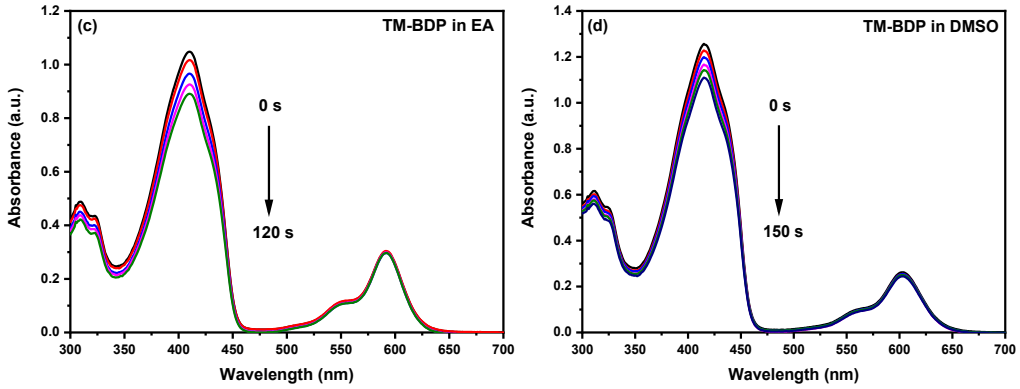

Fig. S17 The singlet oxygen yield test of the TM-BDP in different solvent

4. The singlet oxygen yield test of the TM_2-BDP in different solvent

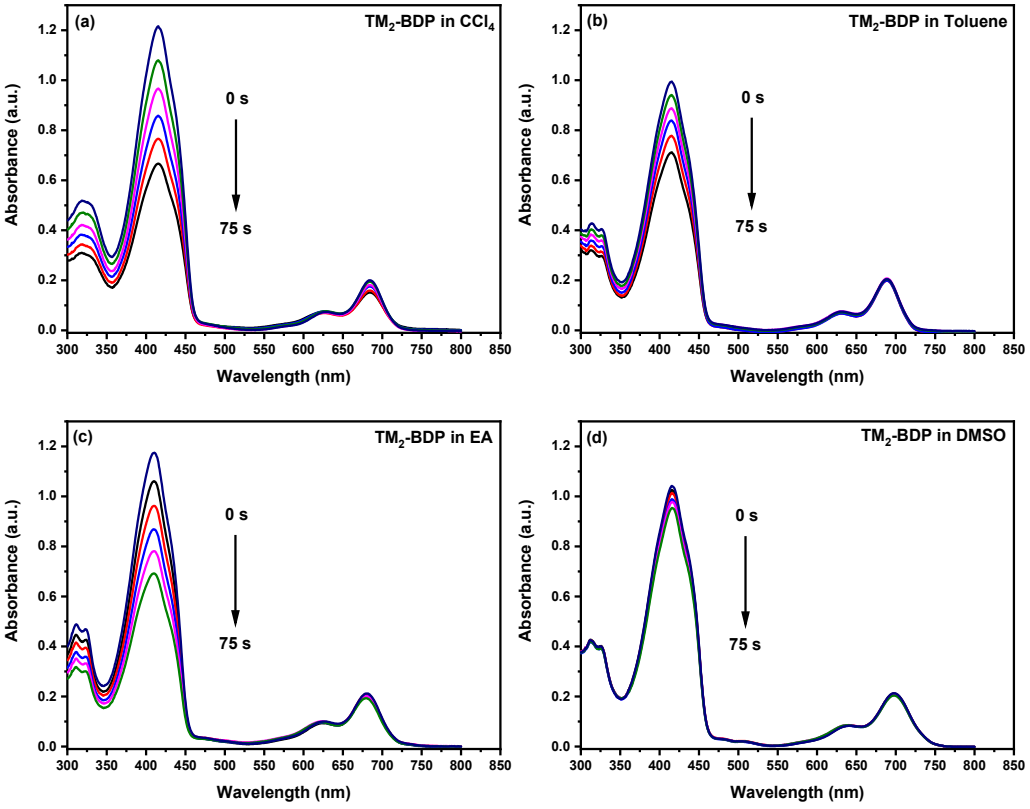

Fig. S18 The singlet oxygen yield test of the TM_2-BDP in different solvent

5. The singlet oxygen yield test of the TM_4-BDP in different solvent

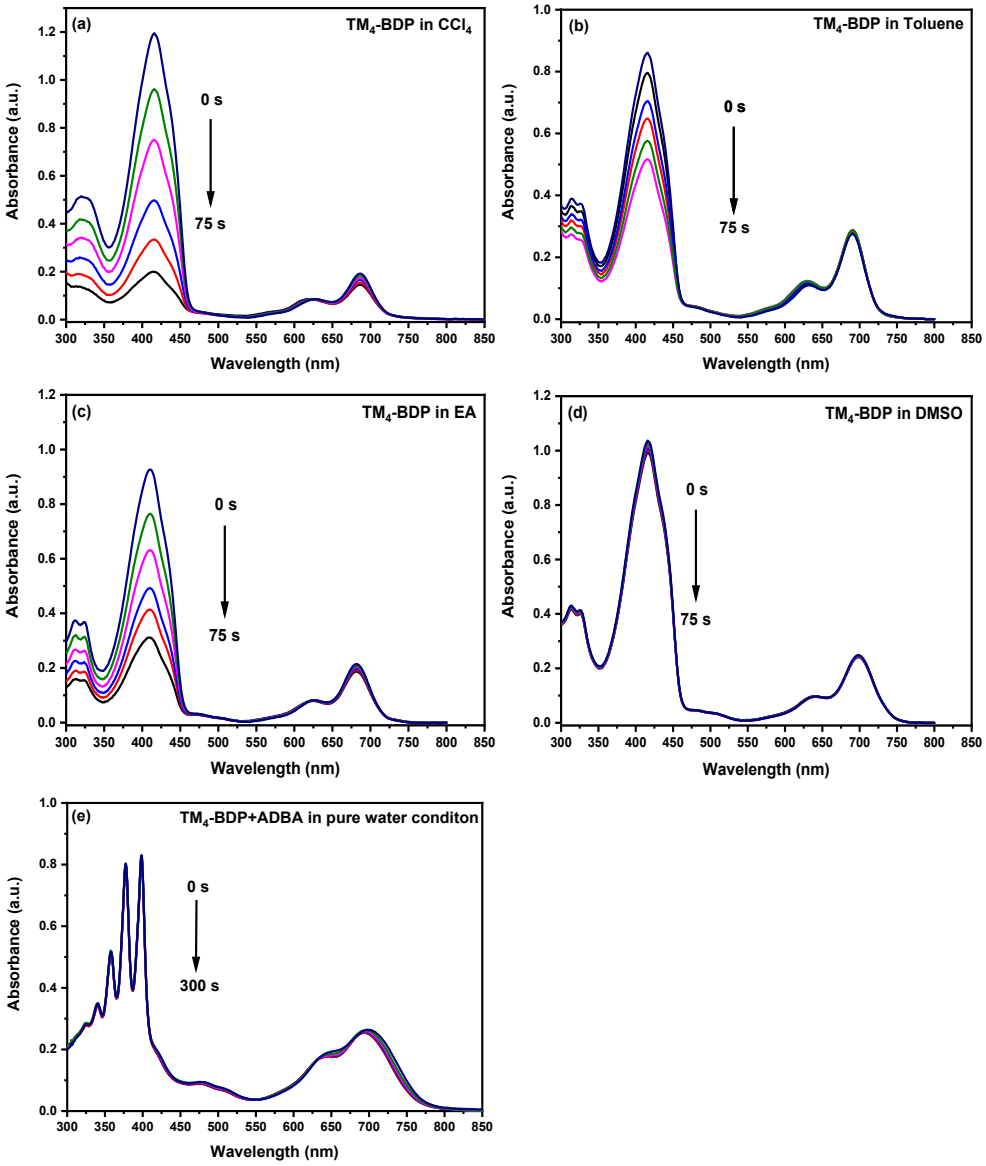

Fig. S19 The singlet oxygen yield test of the TM_4-BDP in different solvent

6. The singlet oxygen yield test of the AM_2-BDP and AM-BDP in dichloromethane solvent

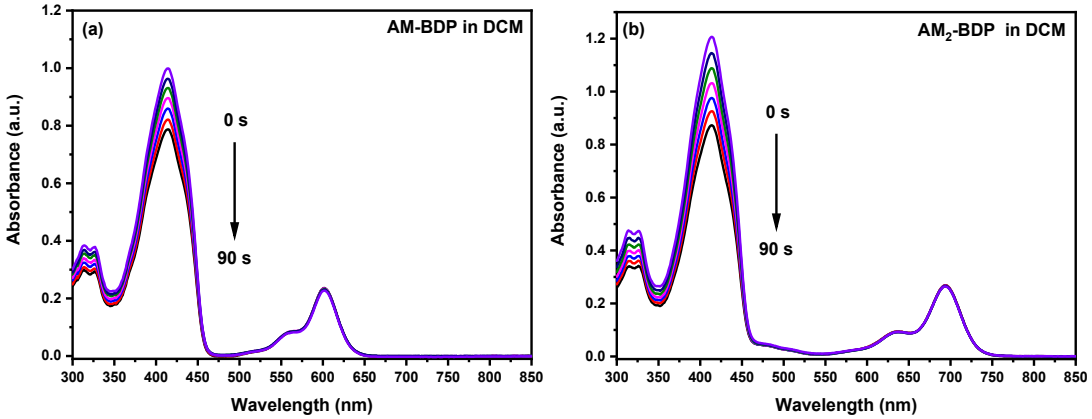

Fig. S20 The singlet oxygen yield test of the AM-BDP and AM_2-BDP in dichloromethane solvent

7. The singlet oxygen yield test of the indocyanine green in CH_3OH and the fluorescence quantum yield test of TM_2-BDP and TM_4-BDP

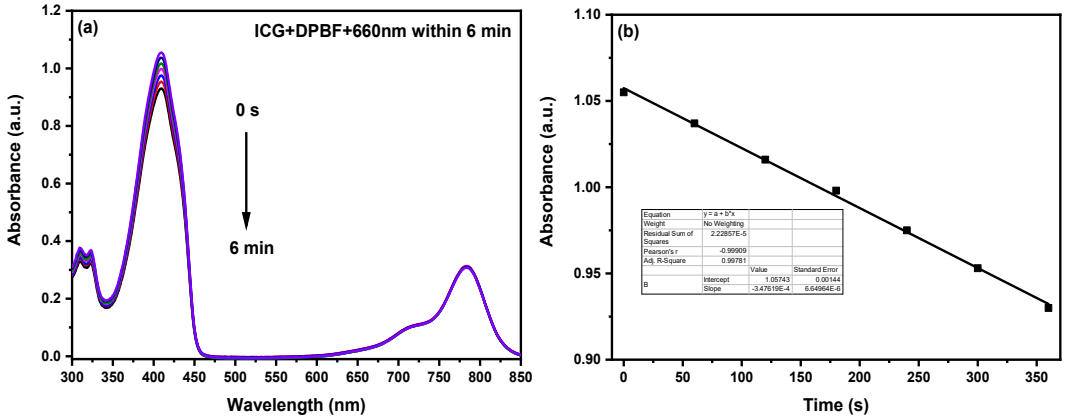

Fig. S21 The singlet oxygen yield test of the indocyanine green in CH_3OH solvent

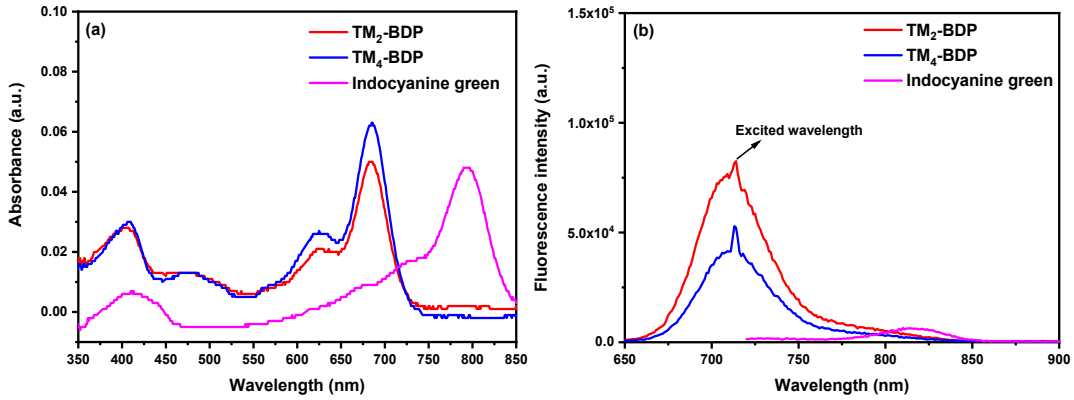

Fig. S22 The fluorescence quantum yield test of TM_2-BDP and TM_4-BDP in DMSO solvent

8. The dihedral angles and electron /hole transfer situation of AM_2-BDP photosensitizer

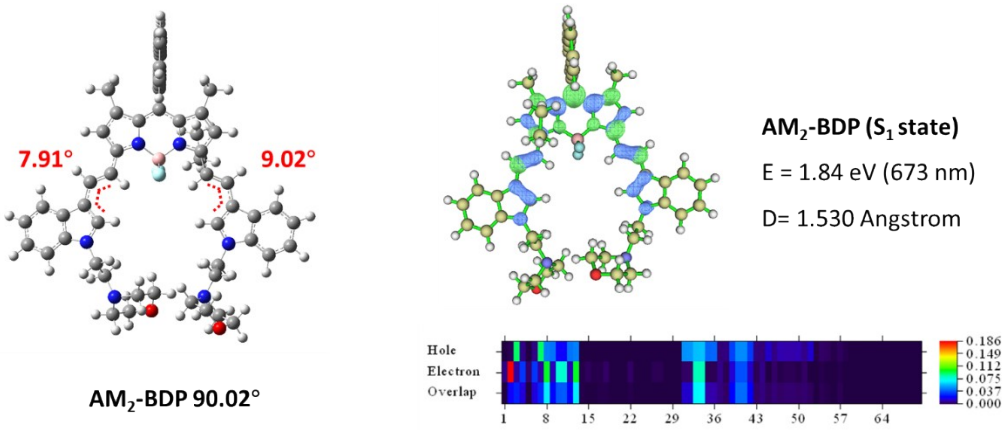

Fig. S23 The dihedral angles and electron/hole transfer situation of AM_2-BDP photosensitizer

9. The transient absorption spectral and attenuation curves of major absorption peaks of the TM_2-BDP photosensitizer

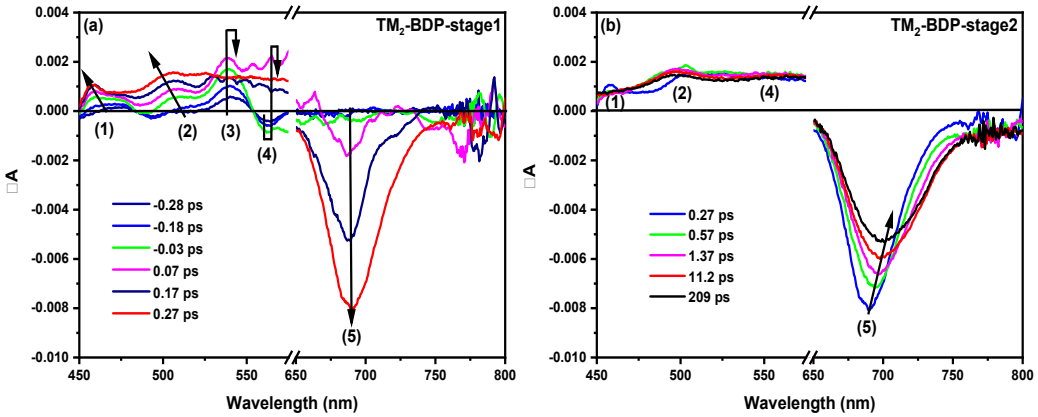

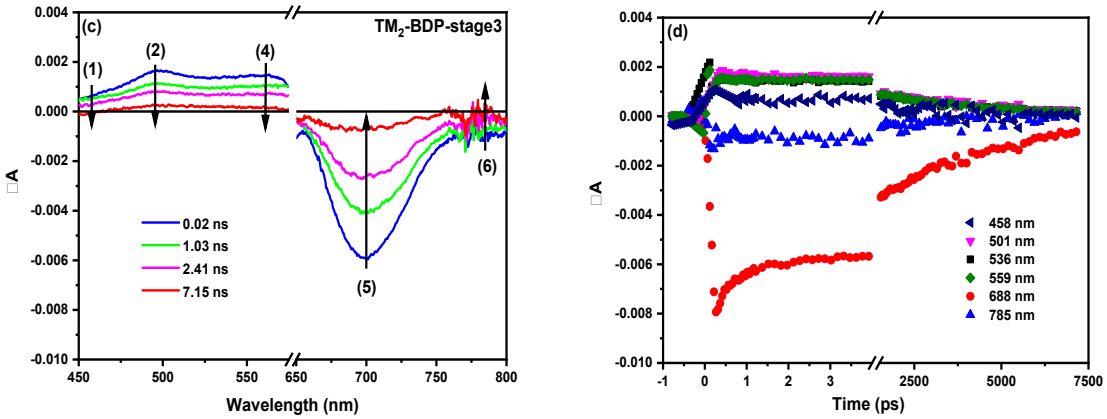

Fig. S24 The transient absorption spectral and attenuation curves of major absorption peaks of the TM_2-BDP photosensitizer.

10. The dihedral angles and electron/hole transfer situation of TM_2-BDP photosensitizer at ground state and S_{1min} state with its' frequency analysis

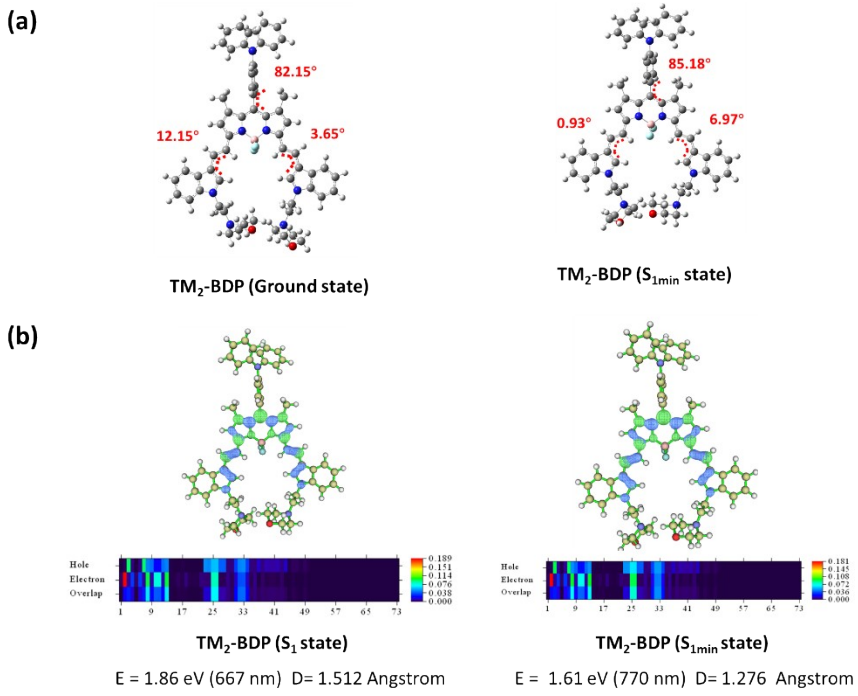

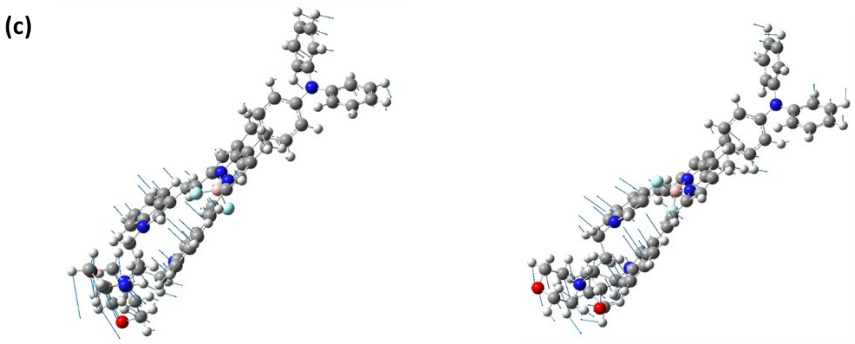

Fig. S25 (a) Dihedral angles of TM_2-BDP photosensitizers at their ground state or S_{1min} state. (b) The electron (green) and hole (blue) transfer situation of TM_2-BDP at their S_1 or S_{1min} state. (The atomic number of the heat map is range from the number of the first non-hydrogen element)(c) The frequency analysis of the TM_2-BDP at its S_{1min} configuration.

11. The triplet excited state information of the TM_4-BDP.

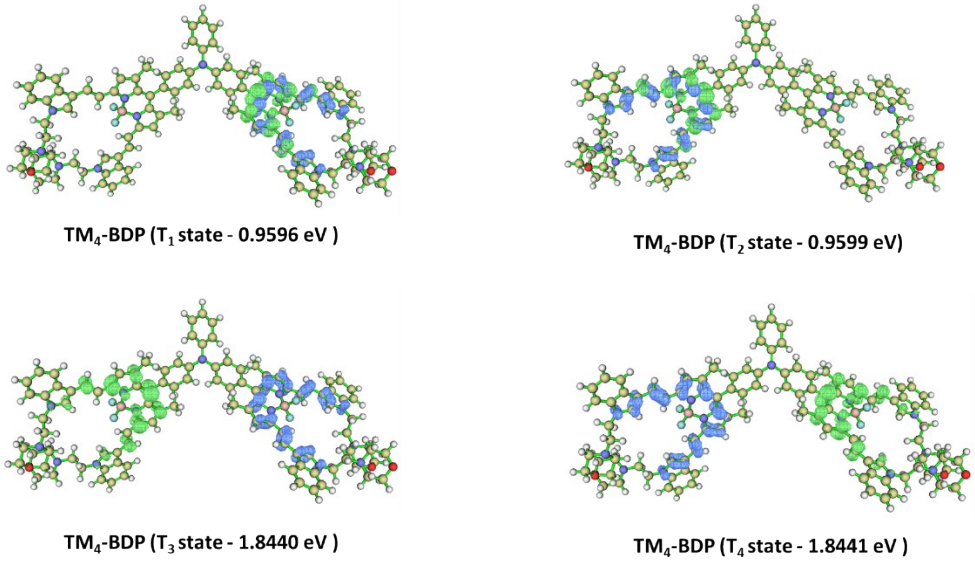

Fig. S26 The electron (green) and hole (blue) transfer situation of TM_4-BDP at T_{1-4} state.

12. The transient absorption spectral and attenuation curves of major absorption peaks of T-BDP photosensitizer

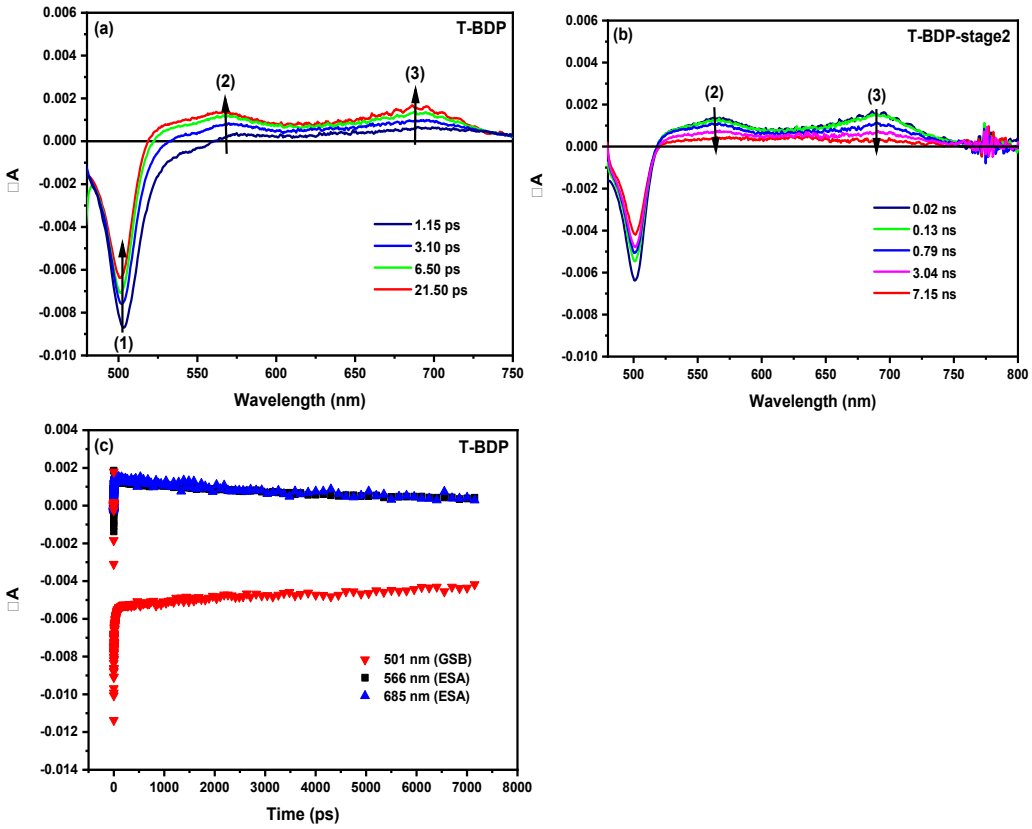

Fig. S27 The transient absorption spectral and attenuation curves of major absorption peaks of the T-BDP photosensitizer.

13. The methods of the theoretical calculations

The geometry optimization and excited state calculation was performed on Gaussian 16 Rev C.01 software through DFT/TD-DFT method at the B3LYP/6-31G(d) level. The DCM solvent in IEFPCM solvent mode was chosen for the theoretical calculation. The MO contribute analysis and the electron-hole transfer situation were analysed with the Multiwfn 3.8 Version software

14. The experiment procedure of singlet oxygen yield test[5], superoxide radical detection[6] and fluorescence quantum yield[7, 8]

Firstly, the absorbance of the photosensitizer was adjusted to about 0.3. Then, the suitable 1,3-Diphenylisobenzofuran(DPBF) solution was added to the above solution and make the absorbance of DPBF near 1.0. Afterward, the mixed solution was exposed to corresponding LED lamp with the main emission wavelength at 660 nm for approximate time interval and the ultraviolet spectra was recorded immediately. Taking the decrease in max absorbance of DPBF as the horizontal coordinate and the time interval as vertical coordinate to obtained the slope(the k value) for the calculation of the singlet oxygen yield. The value of pearson coefficient of fitted line was used to verify whether the concentration of oxygen or DPBF is saturated during the period of experiments. The reference also was tested in the same method. The singlet oxygen quantum yield was calculated according to the following equation with the indocyanine green in CH_3OH as singlet oxygen reference($\boldsymbol{\phi}_{\triangle}$=0.002):

$$\phi_{\triangle} = \phi_r \times \frac{k_s}{k_r} \times \frac{1 - 10^{-OD_r}}{1 - 10^{-OD_s}}$$

Where $\boldsymbol{\phi}_{\triangle}$ represent the singlet oxygen yield, the “r” represent the reference sample, “s” represent the test sample, “k” was the slope of absorbance decrease of DPBF with the time interval and “OD” was stand for absorbance correction factor.

In the superoxide radical test, the 5,5-dimethyl-1-pyrroline N-oxide (DMPO) was used as the chemical indicator of superoxide radical($O_2^{-\cdot}$)[6, 9]. After the mixture of DMPO and TM_4-BDP was illuminated for 4 min, the electron paramagnetic resonance(EPR) spectral was used to capture the signal of superoxide radical($O_2^{-\cdot}$).

In the fluorescence quantum yield test, the indocyanine green in DMSO solution ($\boldsymbol{\phi}$r=0.13) was selected as the reference. The absorbance of both sample and reference was adjusted to about 0.05 for making sure the examined wavelength

region lower than 0.05, then the wavelength at the intersection was used to excite the sample and reference, and the fluorescence quantum yield was calculated by the following formula.

$$\phi_f = \phi_r \times \frac{A_r}{A_s} \times \frac{F_s}{F_r} \times \frac{n_s^2}{n_r^2}$$

Where $\boldsymbol{\phi}_f$ is stand for the fluorescence quantum yield, the "r" represent the reference sample, "s" represent the test sample A is stand for the absorbance, F is stand for integration of fluorescence spectra, n is stand for the refractive index.

15. The experiment procedure of ROS detection under 660 nm [10] and 1000 nm fs-laser excitation in experimental condition

The fluorescence indicator DCFH was used for the detection of total ROS generation. The mixture of DCFH solution (10 μL, 10^{-2}M) and TM_4-BDP(2 μL, $2*10^{-3}$M) in 1 mL pure water solvent was continuously exposed to LED light at 660 nm repeatedly with the same time interval and its fluorescence changes were recorded by fluorescence spectral after each exposure.

The experiment method and dosage for ROS detection under 1000 nm fs laser excitation is basically same with under LED at 660 nm, except that the volume of solvent was reduce to 0.5 mL and the light source was changed to the 1000 nm fs-laser. Besides that, since the efficiency of two-photon excitation at 1000 nm fs-laser is relatively low[18], thus, only the time interval at 30 min was tested for demonstrated the ROS generation ability of TM_4-BDP under two photon excitation.

16. The experiment procedure of light/dark cytotoxicity test[11]

After the cultivation of CNE-2 cells in two 96-well plate (about 1×10^4 cells/well) for 24 h, the photosensitizer with different concentrations (0-24 μM) were added into one of 96- well plate. After another 24 h incubation, the medium tested sample was replaced to remove dead cells and excess photosensitizer. The phototoxic cell experiment group was conducted by irradiating the 96-well plate with red LED light at

660 nm for 30 minutes and the sample for dark toxicity tested still was placed in the incubator during that time. Afterward, after 12 h incubation, the MTT solution (thiazolyl blue ,10 μL; 5 mg/mL) was added into the both two 96-well plates and were incubated at proper environment for 4 h. At last, the MTT solution was replaced with 200 μL DMSO in each well. The absorbance at 570 nm of each well was measured with the enzyme-labeled instrument. The IC_{50} was defined as the concentration of photosensitizer required for a cell inhibition rate of 50%, which was obtained by the linear fitting the photosensitizer concentration and cell inhibition rate, which include at least 6 data point.

Cell viability = (Mean absorbance of test wells – Mean absorbance of medium control wells) / (Mean absorbance of untreated wells - Mean absorbance of medium control wells) ×100%

17. The experiment procedure of fluorescence imaging[12], co-localization experiment [13]，ROS detection[14] and AO/EB staining test[15, 16] in cells

In the cell fluorescence imaging, the CNE-2 cells were seeded into petri dish with 2 mL 1640 culture medium. After 24 h of cell cultivation, 10 μL photosensitizer ($2*10^{-3}$ M) solution was added into the petri dish and incubate with cells for 6 h. Then, after 3 time wash by 2 mL PBS solution, the fluorescence imaging was perform on Olympus FV3000 laser scanning confocal microscope.

In the lysosome co-localization experiment, the Lyso-Tracker Green was used to determined the lysosome localization ability of TM_4-BDP photosensitizer. After 24 h of cell cultivation, 10 μL photosensitizer ($2*10^{-3}$ M) solution was added into the petri dish and incubate with cells for 6 h. Then the 2μL mother liquor of Lyso-Tracker Green was added to that dish and incubate with cells for 1 h. Then, after 3 time wash by 2 mL PBS solution, the fluorescence imaging in two channel was perform on Olympus FV3000 laser scanning confocal microscope. The plot profile analysis and co-localization coefficient was calculated on Image J software.

In the ROS detection experiment, the CNE-2 cells were seeded into petri dish with 2 mL 1640 culture medium. After 24 h of cell cultivation, 10 μL TM_4-BDP

photosensitizer ($2*10^{-3}$ M) solution was added into the petri dish and incubate with cells for 6 h. Once the confocal microscope confirms that the photosensitizer has entered the cell, then, the DCFH-DA (2 μL,10^{-2}M) mother liquor was added into the petri dish and incubate with cells for 20 min in dark condition. After the corresponding irradiated treatment of the cells and 3 times wash by 2 mL PBS solution, the Olympus FV-3000 laser scanning confocal microscope was used to detect the ROS generation. The similar method was used in the control group, only with different condition.

In the intracellular photodynamic experiment, the AO/EB stained experiment was perform on CNE-2 cells and the AO/EB was used to indicate the apoptosis condition of the cells. Firstly, three petri dishes filled with CNE-2 cells were named A,B,C and the following three independent experiment was performed on them respectively. The A petri dish was placed under illumination for 30 min. The 10 μL TM_4-BDP photosensitizer ($2*10^{-3}$ M) was added to B petri dish and incubate for 6 hours. The 10 μL TM_4-BDP photosensitizer ($2*10^{-3}$ M) was added to C petri dish and incubated for 6 h, then, treat with 30 min irradiation. Finally, the 10 time-diluted 5 μL AO and 5 μL EB were added to these three dishes severally and incubated for 5 min at dark condition. Then, according to the excitation wavelength on the instruction manual of AO/EB, the Olympus FV-3000 laser scanning confocal microscope was used to analyzing the apoptosis condition of CNE-2 cells.

18. The experiment procedure of two photon fluorescence imaging experiment[17, 18] of TM_4-BDP in zebrafish under 800 nm excitation

In fluorescence imaging of zebrafish, the purchased zebrafish seedling was incubated in melanin inhibitor containing medium at 28.5℃ environment and zebrafish egg will become fish-shaped within 24-48 hours. Then, the 15 μL TM_4-BDP photosensitizer ($2*10^{-3}$ M) was added to the dish contained ten zebrafishes and 2mL medium. After 6 h incubation, a randomly selected zebrafish was transferred to a high-resolution glass petri dish. Then, 20 μL MS222 anesthetic was added to the glass petri dish and incubated for about 3 minutes. Until no

obvious swimming was observed, the zebrafish was used to fluorescence imaging.

19. The experiment procedure of ROS detection of TM_4-BDP in zebrafish under two-photon excitation

In the ROS detection under two photon excitation, the 15 μL TM_4-BDP photosensitizer ($2*10^{-3}$ M) was added to the dish that contained ten zebrafishes and 2mL medium. After 6 h incubation, the 5 μL mother liquor(10^{-2}M) of the DCFH-DA solution was added to the dish and incubated for 20 min. Then, two zebrafishes were randomly selected and transferred to a high-resolution glass petri dish. After 3 min incubation with 20 μL MS222 anesthetic, one of zebrafish was irradiate with the 800 nm laser for 15 min and another zebrafish was directly taken as the control group. Then, the ROS generation of TM_4-BDP photosensitizer was characterized by the fluorescence change in the single photon channel under excitation at 488 nm.

20. Fitting curve of IC_{50} of the light/dark cytotoxicity test of TM_4-BDP in CNE-2 cells

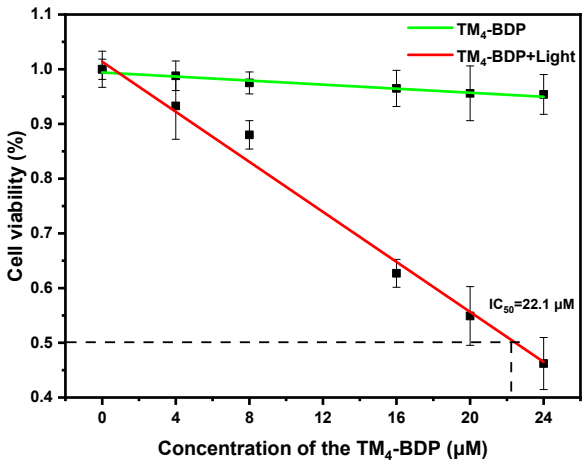

Fig. S28 Fitting curve of IC_{50} value of the light/dark cytotoxicity test of TM_4-BDP in CNE-2 cells

21. The reactive oxygen species detection of TM_4-BDP under 660nm excitation with DCFH as fluorescence indicator in pure water condition

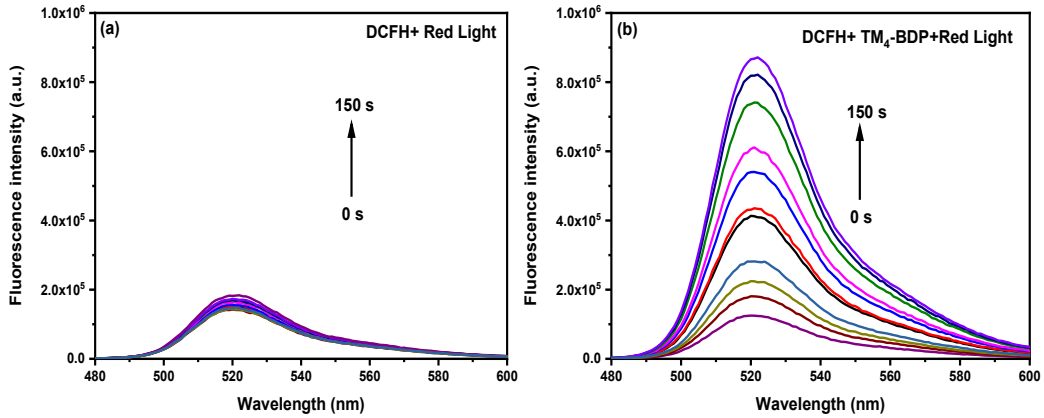

Fig. S29 The reactive oxygen species detection of TM_4-BDP under 660nm excitation with DCFH as fluorescence indicator in pure water condition.

Compared with LED lamps, the efficiency of generating ROS under two-photon excitation is much lower there are two possible reason could be contribute to this phenomenon. The first one is that, as shown in Fig S19(e), the TM_4-BDP could generate singlet oxygen hardly in the pure water condition, which prove the detection of ROS is mainly depend on the generation of superoxide radical. Secondly, the molecule excitation efficiency of two-photon is significantly lower than single-photon way[19], which probably was the main reason for this situation.

22. The light stability test of TM_4-BDP in dichloromethane under 660nm excitation

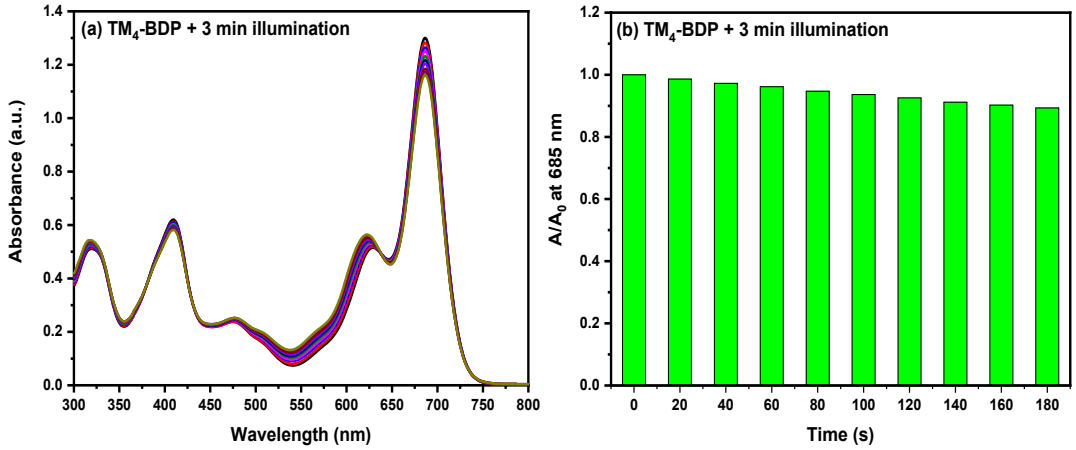

Fig. S30 The light stability test of TM_4-BDP in dichloromethane solvent (The main emission of the LED light was 660 nm and the power density was about 60 mW/cm^2, The A/A_0 mean the absorbance at different illumination time/ the absorbance before illumination, the test concentration of the was 10 μM)

23. Reference:

[1]Wang Z, Zhao J. Bodipy-Anthracene Dyads as Triplet Photosensitizers: Effect of Chromophore Orientation on Triplet-State Formation Efficiency and Application in Triplet-Triplet Annihilation Upconversion. Org Lett, 2017, 19(17): 4492-4495.

[2]Wang Z, Sukhanov AA, Toffoletti A, et al. Insights into the Efficient Intersystem Crossing of Bodipy-Anthracene Compact Dyads with Steady-State and Time-Resolved Optical/Magnetic Spectroscopies and Observation of the Delayed Fluorescence. J Phys Chem C, 2018, 123(1): 265-274.

[3]Wang L, Qian Y. Two effective strategies to improve SOCT-ISC type photosensitizers: Triphenylamine BODIPY with A-D-A configuration and AIE effect and its application in A-549 cells and zebrafish. Dyes Pigm, 2022, 198.

[4]Wang L, Qian Y. Modification of a SOCT-ISC type triphenylamine-BODIPY photosensitizer by a multipolar dendrimer design for photodynamic therapy and two-photon fluorescence imaging. Biomater Sci, 2023, 11(4): 1459-1469.

[5]Zhao X, Yao Q, Long S, et al. An Approach to Developing Cyanines with Simultaneous

Intersystem Crossing Enhancement and Excited-State Lifetime Elongation for Photodynamic Antitumor Metastasis. J Am Chem Soc, 2021, 143(31): 12345-12354.

[6]Li M, Xia J, Tian R, et al. Near-Infrared Light-Initiated Molecular Superoxide Radical Generator: Rejuvenating Photodynamic Therapy against Hypoxic Tumors. J Am Chem Soc, 2018, 140(44): 14851-14859.

[7]Nawara K, Waluk J. Improved Method of Fluorescence Quantum Yield Determination. Anal Chem, 2017, 89(17): 8650-8655.

[8]REFERENCE MATERIALS FOR FLUORESCENCE MEASUREMENT. Pure & Appl Chem, 1988, (7): 1107-1114.

[9]Feng L, Li C, Liu L, et al. Acceptor Planarization and Donor Rotation: A Facile Strategy for Realizing Synergistic Cancer Phototherapy via Type I PDT and PTT. ACS Nano, 2022, 16(3): 4162-4174.

[10]Wan Y, Lu G, Wei WC, et al. Stable Organic Photosensitizer Nanoparticles with Absorption Peak beyond 800 Nanometers and High Reactive Oxygen Species Yield for Multimodality Phototheranostics. ACS Nano, 2020, 14(8): 9917-9928.

[11]Xi D, Xu N, Xia X, et al. Strong pi-pi Stacking Stabilized Nanophotosensitizers: Improving Tumor Retention for Enhanced Therapy for Large Tumors in Mice. Adv Mater, 2022, 34(6): e2106797.

[12]Tian X, Liu T, Zhu M, et al. Endoplasmic Reticulum-Targeting Near-Infrared Fluorescent Probe for CYP2J2 Activity and Its Imaging Application in Endoplasmic Reticulum Stress and Tumor. Anal Chem, 2022, 94(27): 9572-9577.

[13]Dai Y, He F, Ji H, et al. Dual-Functional NIR AIEgens for High-Fidelity Imaging of Lysosomes in Cells and Photodynamic Therapy. ACS Sens, 2020, 5(1): 225-233.

[14]Xiao YF, Chen JX, Li S, et al. Manipulating exciton dynamics of thermally activated delayed fluorescence materials for tuning two-photon nanotheranostics. Chem Sci, 2019, 11(3): 888-895.

[15]He P, Han W, Bi C, et al. Many Birds, One Stone: A Smart Nanodevice for Ratiometric Dual-Spectrum Assay of Intracellular MicroRNA and Multimodal Synergetic Cancer Therapy. ACS Nano, 2021, 15(4): 6961-6976.

[16]Liu K, Liu PC, Liu R, et al. Dual AO/EB staining to detect apoptosis in osteosarcoma

cells compared with flow cytometry. Med Sci Monit Basic Res, 2015, 21: 15-20.

[17]Hammers MD, Taormina MJ, Cerda MM, et al. A Bright Fluorescent Probe for H2S Enables Analyte-Responsive, 3D Imaging in Live Zebrafish Using Light Sheet Fluorescence Microscopy. J Am Chem Soc, 2015, 137(32): 10216-10223.

[18]Addisu KD, Hsu WH, Hailemeskel BZ, et al. Mixed Lanthanide Oxide Nanoparticles Coated with Alginate-Polydopamine as Multifunctional Nanovehicles for Dual Modality: Targeted Imaging and Chemotherapy. ACS Biomater Sci Eng, 2019, 5(10): 5453-5469.

[19]Ming WSaL. Recent Advances in Two-Photon Excited Photodynamic Therapy. Chinese Journal of Lasers, 2022, 49(15).